Scientia Iranica F (2016) 23(3), 1539–1547

Sharif University of Technology
Scientia Iranica
Transactions F: Nanotechnology
www.scientiairanica.com

Effects of elastic contributions on the evolution of nano-structure Al_3Sc phase: A phase-field study

Z. Ebrahimi[a,*] and H. Ebrahimi[b]

a. *Department of Mechanical Engineering, Payame Noor University, Tehran, P.O. Box 19395-3697, Iran.*
b. *Department of Materials Science and Engineering, Sharif University of Technology, Tehran, P.O. Box 11365-9466, Iran.*

Received 21 March 2015; received in revised form 19 December 2015; accepted 13 February 2016

KEYWORDS
Phase-field model;
Al_3Sc precipitates;
Misfit stress;
Coherency.

Abstract. A micromechanical phase-field model is utilized to study the evolution of nano-structure Al_3Sc phase in Al-Sc alloy. We study the formation of Al_3Sc precipitates in an Al-Sc alloy by using an elastic phase-field model. Since the precipitates of Al_3Sc phase are fully coherent with the Al matrix, the elastic energy will have an influence on the resulting morphology. We have studied the effects of elastic strain energies on shape evolution of Al_3Sc phase, numerically. The simulated nano-structures evolve from spherical to cubic shapes. The equilibrium shape of the coherent Al_3Sc phase is found to be determined by minimizing the sum of the elastic and interfacial energies through the phase-field equations. A coherency loss is observed when the precipitates reach a specific size. The simulation results show good agreements with previous experimental studies.

1. Introduction

Due to their light weight, high strength, and corrosion resistance, Al-Sc alloys are of great interest for high-performance structural applications. As a promising and attractive age-hardened aluminum alloy, Al-Sc alloy has been extensively investigated in experimental and numerical studies [1-4]. In binary Al-Sc alloys, Sc additions provide an excellent improvement in mechanical properties owing to the formation of a high-number density of nano-scale $L1_2$-Al_3Sc precipitates during aging [5-8].

In addition of dilute amounts of Sc to Al, the most important intermetallic compound is the Al_3Sc phase. The $L1_2$-Al_3Sc precipitates are coherent with the α-Al matrix with a little lattice misfit of about 1% and form the α-Al/$L1_2$-Al_3Sc interface and a two-phase microstructure. These precipitates have an ordered structure based on the Al fcc lattice with Sc atoms at the face center of unit cells and are very stable with respect to coarsening [8,5]. Due to the similarity between crystal lattice of Al_3Sc phase and the Al matrix in terms of their structures and dimensions, the spherical Al_3Sc phase particles precipitate fully coherently with the matrix during decomposition of solid solution [7]. Therefore, in the decomposition of supersaturated solid solution of Al(Sc), formation of nano-scale Al_3Sc phase and its morphology will depend on elastic energies as well. Therefore, the resulted morphology is determined by the elastic energies and elastic interactions between the precipitates and the matrix. In this paper, we aim to study the elastic contributions in evolution of these phase particles by using a phase-field approach.

The phase-field method has emerged as a powerful tool to predict microstructure evolution in many material systems like coherent solid-state phase transitions [9,10] and multiphase growth [11,12]. It is a genuine representation of the original free-boundary problem in sharp-interface limit as the interface thickness tends to zero. In the phase-field concept, the interfacial conditions are avoided by introducing a set of smooth variables, the so-called phase-field variables,

*. *Corresponding author. Tel./Fax: +98 71 36222255*
E-mail address: z.ebrahimi@pnu.ac.ir (Z. Ebrahimi)

which characterize time and spatial evolutions of bulk phases in the underlying system [13]. The phase-field model has successfully been applied to study the coherent precipitation of $L1_2$ ordered intermetallics from a disordered fcc solid solution in Ni-base alloys [14], in which the formulation of the free energy is based on the concentration wave representation of the ordered state. In a different way, Folch and Plapp have developed a phase-field model for eutectic and peritectic solidification, in which a smooth free energy functional is used to connect any two phase [15]. The work of Folch and Plapp has further been extended to include anisotropic elasticity and misorientations in eutectic growth [16,17], in which the free energy of the system consists of a chemical free energy and an elastic free energy.

Here, the previous elastic phase-field model [16] is first adapted to phase transitions in solids with cubic anisotropy and then applied to model the evolution of Al_3Sc precipitates in an Al-Sc system. This extension of the Folch and Plapp model to precipitate growth is new and has not been reported in the literature. We have represented the related phase-field equations in the first part of this paper. The effects of elastic misfit in precipitation of Al_3Sc particles are discussed later and the simulation results are illustrated.

2. Phase-field model

Consider the precipitate growth in a matrix with an interface of width, W. The distinct entities which should be considered in precipitate growth are the precipitate, the matrix, and the interface between them. Here, we aim to study the formation of Al_3Sc precipitates in an Al-Sc alloy by using an elastic phase-field model. In the phase-field method, we represent the entire microstructure by continuous scalar variables, the so-called phase-field variables, as the volume fraction of the existing phases in the system. Each phase-field variable, which is denoted by ϕ_i, is unity in the corresponding ith single phase region and zero outside that phase, i.e. $\phi_i \in [0,\ 1]$, and smoothly varies between these two values. $\phi_i = 1$ then represents the domain where phase i exists, $\phi_i = 0$ where it is absent, and $0 < \phi_i < 1$ is its bounding interfaces [16]. The phase-field variables should satisfy $\sum_i \phi_i = 1$. In precipitate growth, the index i represents the matrix and the precipitate phases, respectively.

Traditional phase-field models are connected to thermodynamics by a phenomenological free energy functional, written in terms of the phase-field and other fields, such as temperature, concentration, and strain. Through a dissipative minimization of this free energy, the dynamics of one or more order parameters, as well as those of heat or mass transfer are governed by set of non-linear partial differential equations. In phase-field models of coherent binary alloys considered here, the free energy density is a functional of two phase-filed variables, $\vec{\phi} = (\phi_p, \phi_m)$, a concentration, c, a temperature, T, and vector of elastic displacements, $\vec{u}$. The total free energy of the material system is described by the volume integrals of the free energy density, as introduced in [16]:

$$F = \int_V f(\vec{\phi}, c, T, \vec{u}) dV, \tag{1}$$

where the bulk free energy density, $f(\vec{\phi}, c, T, \vec{u})$, is given by:

$$f(\vec{\phi}, c, T, \vec{u}) = \frac{\epsilon_\phi^2 |\vec{\nabla}\vec{\phi}|^2}{2} + H f_p(\phi_i) + X f_{ch}(\phi_i, c, T) + Y f_{el}(\vec{\phi}, \vec{u}), \tag{2}$$

where $\epsilon_\phi = \sqrt{H}W$ is a constant that sets the interface energy and has the unit of energy per unit length, $[J/m]^{1/2}$, and the gradient term on rhs of Eq. (2) is the kinetic part of the free energy density. The constant W sets the length scale of the interface between matrix and precipitate phases. The constants H, X, and Y have the dimension of energy per unit volume $[J/m^3]$.

The dimensionless functions f_p, f_{ch}, and f_{el} must have two local minima to account for two possible phases, which are the matrix m and precipitate phase, p. The elastic interactions are included in the phase-filed model by defining an elastic free energy density, f_{el}, which is described in Eq. (11). The function f_p is the double well potential, which has two minima for ϕ_p and ϕ_m, corresponding to the phase-field variables of the matrix and precipitate phases, respectively. The simplest choice for f_p, which is usually used in the phase-filed models, is:

$$f_p(\phi_i) = \sum_i \phi_i^2 (1 - \phi_i)^2 \quad \text{for } i = m, p. \tag{3}$$

Structural transformations in alloys involve the precipitation of one or more ordered phase from a disordered phase and mass transport. The transformation that we consider here is the precipitation of Al_3Sc phase particles from the Al matrix. Two concentration fields are defined in this case, one for the precipitate phase, c_p, and another for the matrix phase, c_m. The concentrations c_p and c_m are restricted to satisfy a constant chemical potential by imposing the condition $\partial B_p(c_p)/\partial_c = \partial B_m(c_m)/\partial_c$, where B_p and B_m are the free energies of the precipitate and the matrix phases, respectively. This implies that any diffuse interface is a mixture of matrix and precipitate phases with a constant chemical potential.

The function f_{ch} is the chemical free energy density, which determines the phase-diagram of the alloy and is defined as:

$$f_{ch}(\phi_i, c, T) = \frac{1}{2}(c - \sum_i c_i g_i(\phi_i)^2 + \sum_i B_i(T) g_i(\phi_i),$$

$$\text{for } i = m, p, \tag{4}$$

where c_i is the concentration of the phase i in equilibrium with another phase and B_i is the free energy density of phase i.

The relative stability of the phases depends on the concentration values. This requires adding a function to the free energy density that well tilts the double by an amount proportional to the local driving forces [15]. We construct a function, g_i, that well tilts the double and besides keeps the minima of the free energy at fixed values $\phi_i = 0, 1$ independent of the value of c. In other words, $g_i(\phi_i)$ should be a monotonic function satisfying $g_i(\phi_i = 0) = 0$ and $g_i(\phi_i = 1) = 1$. We construct the tilting function, g_i, analogous to the available models of single-phase solidification [18] as follows:

$$g_i(\phi_i) = \phi_i^3(6\phi_i^2 - 15\phi_i + 10), \tag{5}$$

where the index i represents the ith phase region, which could be the precipitate or the matrix phase. We define the chemical potential μ as the variation of F with respect to the concentration c:

$$\mu = \frac{\delta F}{\delta c} = c - \sum_i c_i g_i(\phi_i) \quad \text{for } i = m. \tag{6}$$

The concentration field c evolves according to mass conservation equation:

$$\frac{\partial c}{\partial t} = \vec{\nabla} \cdot \left(M(\vec{\phi}) \vec{\nabla} \frac{\delta F}{\delta c} \right), \tag{7}$$

where $M(\vec{\phi})$ is the chemical mobility. Substituting the chemical potential given by Eq. (6) in Eq. (7), the mass conservation equation becomes:

$$\frac{\partial \mu}{\partial t} = \vec{\nabla} \cdot \left(D(\vec{\phi}) \vec{\nabla} \mu \right) - \sum_i c_i \frac{\partial g_i(\phi_i)}{\partial t}, \tag{8}$$

where $D(\vec{\phi}) = XM(\vec{\phi})$ is a phase-dependent diffusivity. In our model, we consider the diffusivity as $D(\vec{\phi}) = D\phi_m$, where D is the solute diffusion coefficient.

To describe the elastic stresses in evolution of coherent precipitates, we consider uni-directional misfit applied on the interface of two different solid phases. The misfit strain ϵ_m accommodates the misfit stress σ_{ij}^m on the boundary between two solid phases as described in [16]. The constitutive law for a material with cubic-anisotropy is established by only 3 material constants, C_{11}, C_{12}, and C_{44}. In two-dimensional model, the displacement vector is $\vec{u} = (u_1, u_2)$ and the stress and the strain tensors are $\vec{\sigma} = (\sigma_{11}, \sigma_{22}, 2\sigma_{12}$ and $\vec{\epsilon} = (\epsilon_{11}, \epsilon_{22}, 2\epsilon_{12})$, respectively. We write a general stress-strain relation according to linear elasticity to relate the stress and strain tensors, σ_{ij} and ϵ_{ij}, respectively:

$$\epsilon_{ij} = \frac{1}{2} \left(\frac{\partial u_i}{\partial x_j} + \frac{\partial u_j}{\partial x_i} \right), \tag{9}$$

$$\sigma_{ij}^s = c_{ijkl}^s \epsilon_{kl} - \sigma_{ij}^m \delta_{ij}, \quad s = m, p, \tag{10}$$

where $i, j = 1, 2$ in our phase-field model.

The elastic free energy $f_{el}(\vec{\phi}, \vec{u})$, which incorporates the elastic interactions due to the lattice misfit between the precipitate and the matrix phases in the phase-field model, is defined as:

$$f_{el} = \sum_{s=m,p} h(\phi_s) f_{el}^s, \tag{11}$$

$$f_{el}^s = \frac{1}{Y} c_{ijkl}^s (\epsilon_{kl} - \epsilon_m \delta_{ij})^2, \tag{12}$$

where c_{ijkl} is the forth-order stiffness tensor. The phase-dependent elastic free energy density of the system f_{el} is constructed by the sum of the elastic free energy densities of individual phases f_{el}^s weighted by a function $h(\phi_s)$. We choose $h(\phi_s) = \phi_s^2(3 - 2\phi_s)$, which satisfies $h(\phi_s = 1) = 1$, $h(\phi_s = 0) = 0$ and $h'(\phi_s = 0, 1) = 0$. The misfit strain ϵ_m is included in Eq. (12) to incorporate the influence of the misfit between eutectic lamellae.

The temporal evolution of the two non-conserved phase-field variables ϕ_m and ϕ_p gives the location of interface between the precipitate and the matrix phases and is a relaxation toward the minimum of the free-energy functional F:

$$\tau(\vec{\phi}) \frac{\partial \phi_i}{\partial t} = -\frac{1}{H} \frac{\delta F}{\delta \phi_i}|_{\phi_m + \phi_p = 1}, \quad \text{for } i = m, p. \tag{13}$$

$\tau(\vec{\phi})$ is a relaxation time and controls the time of attachment of atoms to solid interfaces. Since we have the constraint $\phi_p + \phi_m = 1$ in our phase-field model, we can consider the equation of motion (Eq. (13)) for the precipitate phase only. The evolution of the matrix phase is then computed as $\phi_m = 1 - \phi_p$. The derivative $\delta F / \delta \phi_i|_{\phi_p + \phi_m} = 1$ in Eq. (13) can be evaluated by the method of Lagrange multipliers analogous to [15]. Using this and replacing the components of the free energy density, f_p (Eq. (3)), f_{ch} (Eq. (4)), and f_{el} (Eq. (11)) in Eq. (13), we obtain the evolution of ϕ_p as:

$$\begin{aligned} \tau(\vec{\phi}) \frac{\partial \phi_p}{\partial t} =& W_\phi^2 \nabla^2 \phi_p - 2\phi_p(1 - \phi_p)(1 - 2\phi_p) \\ & - \frac{\lambda_c}{2} \frac{\partial g_p(\phi_p)}{\partial \phi_p} [\mu(c_m - c_p) - (B_m - B_p)] \\ & - \frac{\lambda_e}{3} \left[2 \frac{\partial h(\phi_p)}{\partial \phi_p} f_{el}^p - \frac{\partial h(\phi_m)}{\partial \phi_m} f_{el}^m \right], \end{aligned} \tag{14}$$

By taking the derivatives $\partial g(\phi_p)/\partial\phi_p$ and $\partial h(\phi_p)/\partial\phi_p$, Eq. (15) is then simplified to:

$$\tau(\vec{\phi})\frac{\partial\phi_p}{\partial t} = W_\phi^2\nabla^2\phi_p - 2\phi_p(1-\phi_p)(1-2\phi_p) - 15\lambda_c\phi_p^2(1-\phi_p)^2[\mu(c_m-c_p) - (B_m-B_p)] - 2\lambda_e[2\phi_p(1-\phi_p)f_{el}^p - \phi_m(1-\phi_m)f_{el}^m], \quad (15)$$

where $W = \epsilon_\phi/\sqrt{H}$ is the thickness of the interface between the precipitate and the matrix phase. $\lambda_c = X/H$ is a coupling constant that connects the phase-field model to the material parameters and the phase-diagram of the alloy. The constant $\lambda_e = Y/H$ also couples the elastic interactions to the phase-field equation.

We evaluate the elastic displacements (u_1, u_2) by a set of nonlinear equations, which are obtained by writing the mechanical equilibrium equation within the alloy system:

$$\frac{\partial}{\partial x_j}\left(\sum_s h(\phi_s)\sigma_{ij}^s\right) = 0 \quad \text{for } s = m, p. \quad (16)$$

An elastic phase-field model with cubic-anisotropy for eutectic solidification is developed in [16]. We modify this model to account for elastic interactions in precipitation of Al_3Sc phase from the Al matrix. The elastic free energy of the individual phases in Eq. (12) for cubic-anisotropy is given by:

$$f_{el}^s = \frac{1}{Y}[(C_{11}^s + C_{12}^s)(\epsilon_{11}^2 + \epsilon_{22}^2) + 2\epsilon_{12}^2 C_{44}^s + - 2\epsilon_m^2(C_{11}^s + C_{12}^s) - 2\epsilon_m(C_{11}^s + C_{12}^s)(\epsilon_{11} + \epsilon_{22})]. \quad (17)$$

Substituting σ_{ij} and ϵ_{ij} from Eqs. (10) and (9) in Eq. (16) and taking the derivatives for $i, j = 1, 2$, results in a system of two differential equations in terms of the displacement fields, u_1 and u_2 (see Ref. [16] for more details). Once the displacements are found by solving Eq. (16), the corresponding strains are computed from the linear elasticity theory, Eq. (9). After that, the calculated components of the strain tensor will be substituted in the phase-field evolution equation (Eq. (15)). The phase-filed equation is solved together with the diffusion equation (Eq. (8)) and the phase-filed variables ϕ_p and ϕ_m and the concentration c are evaluated at each time step.

3. Numerical simulations

3.1. Model parameters

We consider a supersaturated Al-Sc solid solution, which can decompose via a precipitation reaction to form coherent precipitates of the Al_3Sc phase. In our phase-field model, the temperature is kept constant when an isolated precipitate of phase p is growing into a matrix of phase m. The compositions of Al matrix and Al_3Sc precipitates are normalized in such a way that the scaled equilibrium composition of phase m is zero and that of phase p is one. The radius of the particle precipitates is r_0 with composition of c_p. The initial composition outside the particle is c_∞. We define the matrix supersaturation parameter (equilibrium volume fraction) as $\eta = (c_\infty - c_m)/(c_p - c_m)$, where c_m is the equilibrium matrix composition obtained from phase diagram and the precipitates grow under a supersaturation of $(c_\infty - c_m)$. We use estimated values of $D = 5.2\times10^{-4}$ m^2/s and $\eta = 0.1$ for the simulations.

Uniaxial compression tests of Al-Sc alloy show that the Al_3Sc intermetallic compound is harder than pure Al phase. The mechanical properties of $L1_2$-Al_3Sc precipitates are widely investigated [19,20]. The used values of the elastic constants of the precipitates and the matrix are listed in Table 1. As in the standard phase-field models [18], the interface thickness W should be larger than the average capillary length, $\bar{d}$, to make the phase-field simulations feasible. Therefore, we choose $W/\bar{d}$ as the resolution for our model in a way that it fulfills the above requirement. We define the phase-dependent relaxation time as:

$$\tau(\vec{\phi}) = \bar{\tau} + \frac{\tau_m - \tau_p}{2}\left(\frac{\phi_m - \phi_p}{\phi_m + \phi_p}\right), \quad (18)$$

where τ_i $(i = m, p)$ is the time relaxation of each individual phase and $\bar{\tau} = (\tau_m + \tau_p)/2$. We scale lengths by W and time by $\bar{\tau}$ and get the following dimensionless parameters:

$$\tilde{\tau}(\vec{\phi}) = \frac{\tau(\vec{\phi})}{\bar{\tau}}, \quad \tilde{D} = \frac{D\bar{\tau}}{W^2} \quad \text{and} \quad \tilde{t} = \frac{t}{\bar{\tau}}. \quad (19)$$

The elastic coupling constant λ_e is fixed by $\lambda_e = \lambda_c$ so that $Y = X$.

We use a standard finite difference approach to discretize the model equations with a grid spacing $\Delta x/W = 0.8$. The time-independent mechanical equilibrium equations, Eq. (16), are solved together with the phase field and the diffusion equations, Eqs. (15) and (8), which are simulated by a first-order Euler Scheme with a time step $\Delta t/\bar{\tau} = 0.06$.

A series of two-dimensional simulations are performed in a rectangular box with symmetric boundary conditions. The simulations are started with several

Table 1. Elastic constants for pure Al and Al_3Sc phase as reported in [8].

	C_{11}	C_{12}	C_{44}	A_d
Al	108	61.3	28.5	1.21
Al_3Sc	189	43	66	0.9

spherical precipitates of initial radius r_0 and composition of c_p. We choose the input parameters $W/\bar{d} = 15.085$ and $Y = X = 14.22$ MPa. The coupling constants $\lambda_c = \lambda_e$ are set to 14.26.

3.2. Results and discussions

A series of runs with five precipitate particles of initial radius $r_0 = 2$ nm are performed to examine the evolution of Al_3Sc phase. One of these particles is placed in the center of the simulation box and one in each corner. All of the particles initially have the same size. The misfit strain is set to $\epsilon_m = 0.0125$, as reported in [8]. Figure 1 shows the morphology of the Al_3Sc precipitates after 16000, 38000, and 48000 time cycles. The shape variations of the coherent precipitates are understood by comparing these pictures. As we can see, the precipitate particles evolve from a spherical shape to cubic shapes, Figure 1(a). According to experimental investigations of Al_3Sc evolution [8], coherency loss usually occurs when the precipitate size is large enough. For precipitate radius greater than 20 nm, misfit dislocations are observed, which result in coherency loss, while precipitates with 5 nm of size are coherent [8]. Marquis et al. [8] have observed loss of coherency, detected from the presence of interfacial dislocations, when the precipitate size reaches about $d_{cr} = 40$ nm in diameter, where d_{cr} is defined as a critical diameter for loss of coherency. In the presented simulation, we have imposed the perfect coherency between the Al and Al_3Sc phases until the end of the simulation time. The precipitate cuboids in Figure 1(a) have about 40 nm size. After that cuboids reach this critical value in diameter, a change in the precipitates' shape of trapezoids is observed, Figure 1(b) and (c), which is not a usual shape in precipitate growth. This morphology change can be interpreted as the influence of the coherency strain between the matrix and precipitates, which is still applied in the phase-field model after that the cuboidal size reaches d_{cr}. This verifies the founding about coherency loss of precipitates reported in [8]. Therefore, a loss of coherency should be imposed on the model after a specific time.

To elucidate the effects of strain energy on precipitate evolution, we have performed a series of runs with different misfits, ϵ_m. The initial conditions are the same as those of the previous simulation. Figure 2 represents the morphology of Al_3Sc phase after 8000 time steps for $\epsilon = 0.01$, 0.02, and 0.04. For $\epsilon_m = 0.01$, cuboidal precipitates are observed, while for larger values of misfit, i.e. $\epsilon_m = 0.04$ and 0.06, the cuboidal shapes are changed to some trapezoids and some cup-like structures, respectively. This means that the increase in precipitates radius is accelerated with increasing the misfit parameter. Therefore, the elastic interactions play a role in the evolution of precipitates.

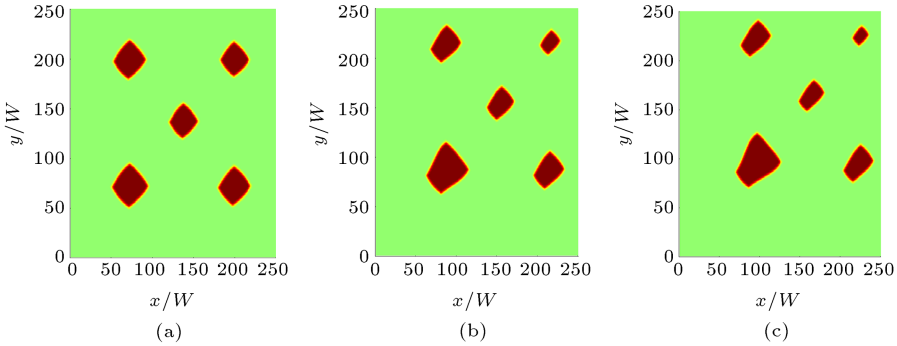

Figure 1. Evolution of the Al_3Sc precipitate in Al-Sc alloy with $\epsilon_m = 0.0125$. The microstructure at (a) $t = 16000$ cycles, (b) $t = 38000$ cycles, and (c) $t = 48000$ cycles.

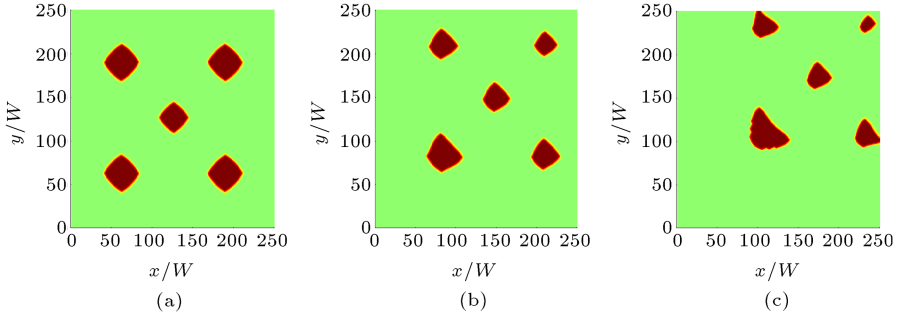

Figure 2. Effects of misfit strain on evolution of the Al_3Sc precipitate in Al-Sc alloy at $t = 8000$ cycles: (a) $\epsilon_m = 0.01$, (b) $\epsilon_m = 0.02$, and (c) $\epsilon_m = 0.04$.

We have also calculated the elastic stress and displacements in the evolution of Al_3Sc phase. The elastic displacements u_1 and u_2 are obtained by solving the mechanical equilibrium equation, Eq. (16). Figure 3 shows the displacements u_1 and u_2 for $\epsilon_m = 0.0125$ at $t = 8000$ cycles. The components of stress tensor are given in Eq. (10). The normal stress σ_{11} is illustrated in Figure 4(a). In Figure 4(b), we have plotted the three

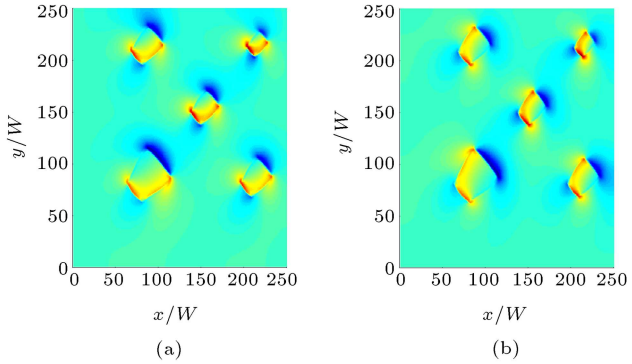

Figure 3. Elastic displacements in evolution of Al_3Sc precipitate at $t = 8000$ cycles and $\epsilon_m = 0.0125$: (a) The displacements u_1; and (b) the displacement u_2.

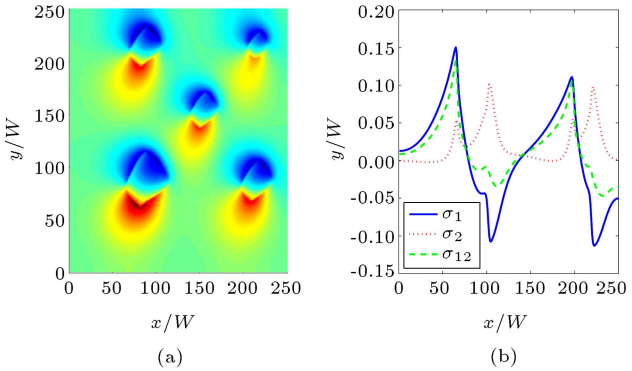

Figure 4. (a) The stress component σ_{11} in evolution of Al_3Sc precipitate with $\epsilon_m = 0.0125$. (b) The plot of three stress components.

stress components σ_{11}, σ_{12}, and σ_{22} along $y/W = 100$, where the interface of the precipitates and the matrix is demonstrated by a sharp change in stress values (from positive to negative values). The normalized value of σ_{11} changes between -0.11 to 0.15 between the precipitates and the matrix; that of σ_{22} varies from -0.03 to 0.1, and σ_{12} from zero to 0.1.

Formation of coherent rod-like precipitates of Al_3Sc has been reported in some experimental studies [8,5]. Therefore, we have performed some simulations of precipitate particles organized in an array. Figure 5 illustrates the evolution of an array of Al_3Sc precipitates with $\epsilon_m = 0.0125$. The rod-like nanostructure after 8000, 24000, and 36000 time steps is presented in this figure. The initial spherical particles of Al_3Sc with radius of $r_0 = 2$ nm evolve to cuboids, Figure 5(a). One can see that the cuboids at the ends of the rod have the largest size, while those in the middle of the rod have the smallest diameter. This diameter variation is due to the coherency between the Al_3Sc precipitates and Al matrix and one can understand that elastic interactions between these closely spaced precipitates play a role.

When the first cuboid in the array reaches about 40 nm in diameter, its shape changes to trapezoid (Figure 5(b)). After that, the height of this trapezoid increases in time. Since formation of trapezoid precipitates is not reported in the literature, we can conclude that a coherency loss is required when the precipitate size reaches a specific value. Another interesting observation in Figure 5 is that the smallest cuboid (the third one from the top) has retained its cubic shape during the simulation. This also verifies the dependence of the elastic interactions on precipitate's size during the evolution of Al_3Sc phase.

The effect of misfit strain on evolution of rod-like structures of Al_3Sc is shown in Figure 6, where the array of precipitates is evaluated for three values of misfits, $\epsilon_m = 0.01$, 0.02, and 0.04. The acceleration

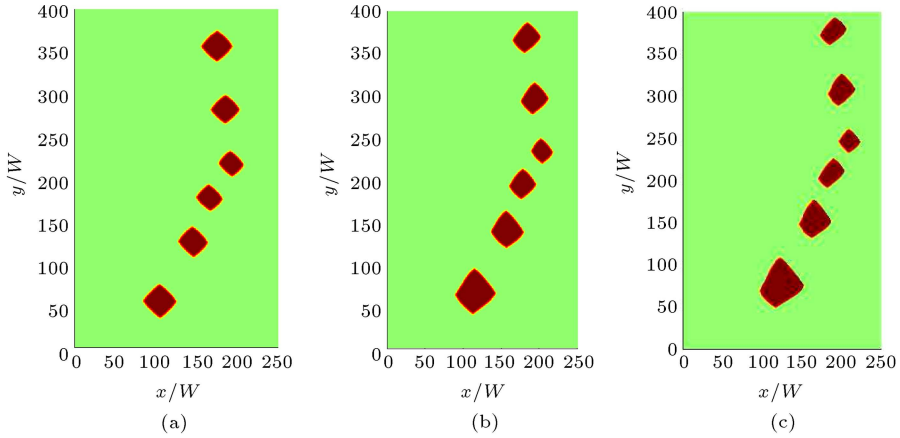

Figure 5. Evolution of Al_3Sc and array of cuboidal precipitates in Al-Sc alloy with $\epsilon_m = 0.0125$. The microstructure at (a) $t = 8000$ cycles, (b) $t = 24000$ cycles, and (c) $t = 36000$ cycles.

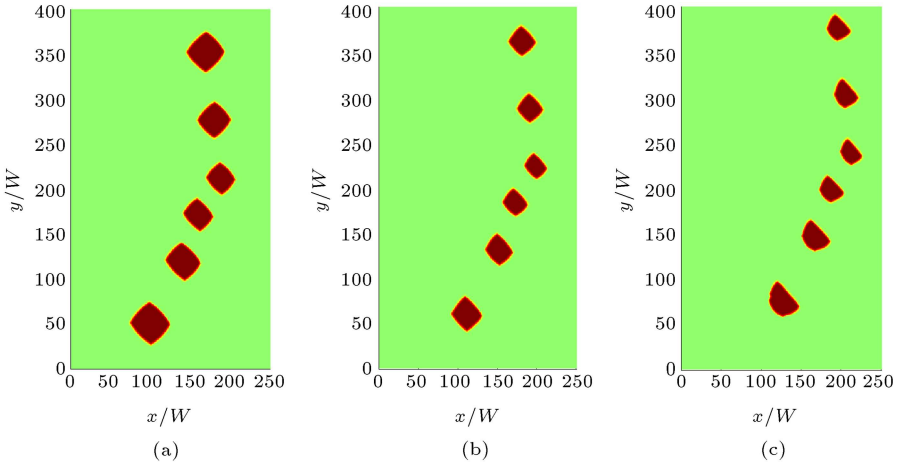

Figure 6. Effects of misfit strain on evolution of the rod-like Al_3Sc precipitates. The array of cuboidal precipitates in Al-Sc alloy is presented: (a) $\epsilon_m = 0$; (b) $\epsilon_m = 0.02$; and (c) $\epsilon_m = 0.04$.

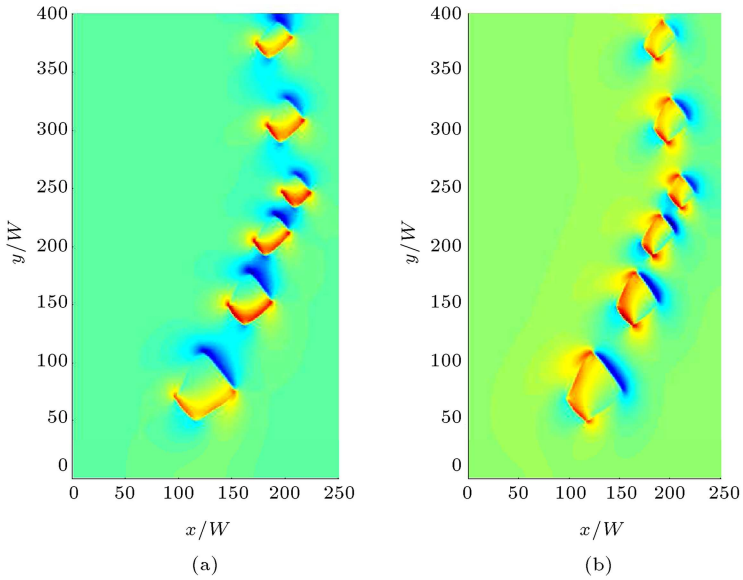

Figure 7. Elastic displacements in an array of cuboidal Al_3Sc precipitates with $\epsilon_m = 0.0125$: (a) The displacements u_1; and (b) displacement u_2.

of growth kinetics with increasing the misfit strain is observed here as well.

At the end of the presented study, we have evaluated the mechanical displacements and stresses in the rod-like structure. The two displacements u_1 and u_2 are illustrated in Figure 7 for $\epsilon_m = 0.0125$. The normal stresses, σ_{11} and σ_{22}, for the same simulation are shown in Figure 8(a) and (b), respectively. Stress components are plotted along the line $y/W = 100$ in Figure 8(c).

Finally, the effect of misfit strain on normal stress σ_{11} in the rod-like structure is investigated. Three runs with $\epsilon_m = 0.02$, 0.04, and 0.06 are carried out and the corresponding stress fields are plotted in Figure 9. Obviously, the value of σ_{11} increases with increasing the misfit strain. Hence, the elastic interactions between the precipitates and the matrix will increase.

4. Summary and conclusion

We have used an elastic phase-field model to investigate the evolution of nano-structure Al_3Sc precipitates in Al-Sc alloy. The effects of elastic interactions on formation of Al_3Sc precipitates have been studied. The simulation results have detected a coherency loss after that the precipitates size reaches a specific value, which is in agreement with previous experimental studies. We have also shown that elastic energy plays a role in evolution of the Al_3Sc phase. We have observed that the spherical precipitates are changed to cuboids due to the coherency between the matrix and the precipitates. The rod-like structures of Al_3Sc phase

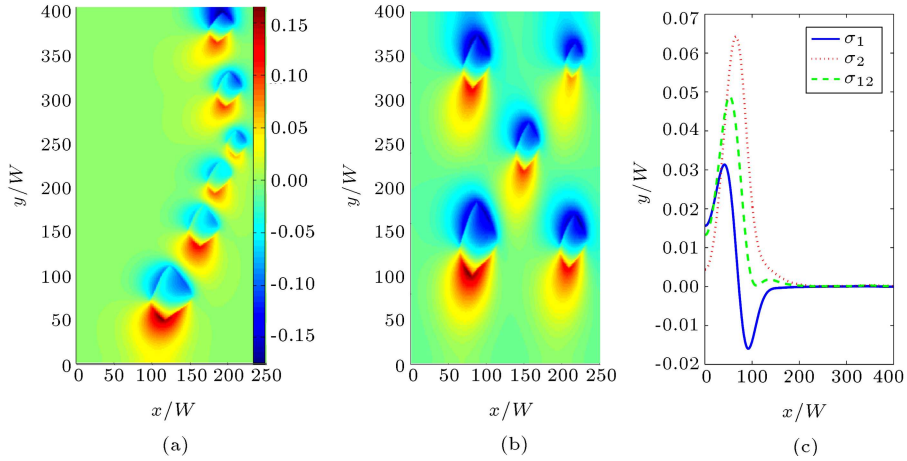

Figure 8. (a) and (b) The stress components of σ_{11}, and σ_{22}, respectively, in evolution of Al_3Sc precipitate with $\epsilon_m = 0.0125$. (c) The plot of three stress components.

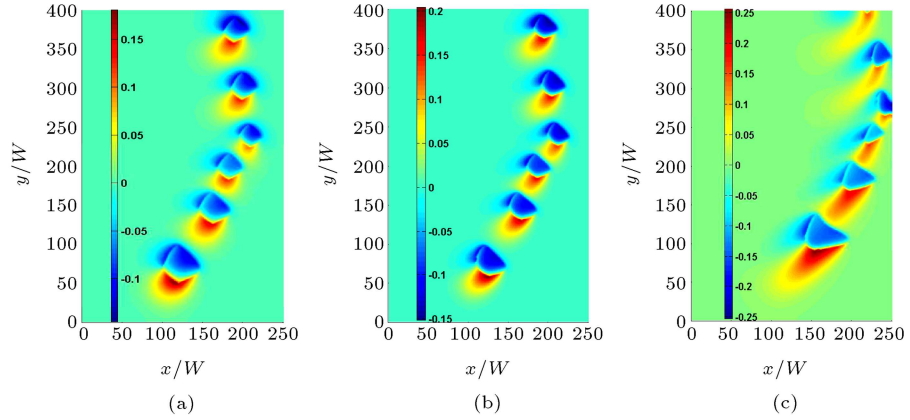

Figure 9. The effect of misfit strain on stress component σ_{11}: (a) $\epsilon_m = 0.02$; (b) $\epsilon_m = 0.04$; and (c) $\epsilon_m = 0.06$.

have also been investigated in this study. Finally, the effects of misfit strain on the array of cuboids and the related stress components and elastic displacements have been evaluated.

References

1. Phillips, M.A., Clemens, B.M. and Nix, W.D. "Microstructure and nanoindenta- tion hardness of Al/Al_3Sc multilayers", *Acta Mater.*, **51**, pp. 3171-3184 (2003).
2. Jindal, V., De, P.K. and Venkateswarlu, K. "Effect of Al_3Sc precipitates on the work hardening behavior of aluminumscandium alloys", *Mater. Lett.*, **60**, pp. 3373-3375 (2006).
3. Fazeli, F., Poole, W.J. and Sinclair, C.W. "Modeling the effect of Al_3Sc precipitates on the yield stress and work hardening of an AlMgSc alloy", *Acta Mater.*, **56**, pp. 1909-1918 (2008).
4. Haidemenopoulos, G.N., Katsamas, A.I. and Kamoutsi, H. "Thermodynamics-based computational design of Al-Mg-Sc-Zr Alloys", *Metall. and Mater., Trans. A*, **41A**, pp. 888-899 (2010).
5. Norman, A.F., Prangnell, P.B. and McEWEN, R.S. "The solidification behavior of dilute aluminum-scandium alloys", *Acta Mater.*, **46**(16), pp. 5715-5732 (1998).
6. Novotny, G.M. and Ardell, A.J. "Precipitation of Al_3Sc in binary AlSc alloys", *Mater. Sci. and Eng., A*, **318**, pp. 144-154 (2001).
7. Davydov, V.G., Rostova, T.D., Zakharov, V.V., Filatov, Y.A. and Yelagin V.I. "Scientific principles of making an alloying addition of scandium to aluminum alloys", *Mater. Sci. and Eng., A*, **280**(1), pp. 30-36 (2000).
8. Marquis, E.A. and Seidman, D.N. "Nanoscale structure evolution of Al_3 Sc precipitates in Al(Sc) alloys", *Acta Mater.*, **49**, pp. 1909-1919 (2001).
9. Fratzl, P., Penrose, O. and Lebowitz, J.L. "Modeling of phase separation in Alloys with coherent elastic misfit", *J. of Stat. Phy.*, **95**(5), pp. 1429-1503 (1999).
10. Thornton, K., Agren, J. and Voorhees, P.W. "Modeling the evolution of phase boundaries in solids at the meso- and nano-scales", *Acta Mater.*, **51**, pp. 5675-5710 (2003).

11. Echebarria, B., Folch, R., Karma, A. and Plapp, M. "Quantitative phase-field model of alloy solidification", *Phys. Rev. E*, **70**, p. 061604 (2004).

12. Tiaden, J., Nestler, B., Diepers, H.J. and Steinbach, I. "The multiphase-field model with an integrated concept for modeling solute diffusion", *Physica D.*, **115**, pp. 73-86 (1998).

13. Qin, R.S. and Bhadeshia, H.K. "Phase field method", *Mater. Sci. and Technol.*, **26**(7), pp. 803-811 (2010).

14. Wang, Y., Banerjee, D., Su, C.C. and Khachaturyan, A.G. "Field kinetic model and computer simulation of precipitation of L1 2 ordered intermetallics from f.c.c. solid solution", *Acta Mater.*, **46**(9), pp. 2983-3001 (1998).

15. Folch, R. and Plapp, M. "Quantitative phase-field modeling of two-phase growth", *Phys. Rev. E*, **72**, p. 011602 (2005).

16. Ebrahimi, Z., Rezende, J.L. and Kundin, J. "Phase-field modeling of microelastically controlled eutectic lamellar growth in a TiFe system", *J. of Cryst. Growth*, **349**, pp. 36-42 (2012).

17. Ebrahimi, Z., Rezende, J.L. and Emmerich, H. "Phase-field modeling of Eu- tectic growth in a Ti-Fe system with multiple nuclei and misorientations", *Metall. Mater. Trans. A*, **44**, pp. 1925-1936 (2013).

18. Karma, A. and Rappel, W.J. "Quantitative phase-field modeling of dendritic growth in two and three dimensions", *Phys. Rev. E*, **57**, pp. 4323-4349 (1998).

19. Duan, Y.H., Sun, Y., Peng, M.J. and Zhou, S.G. "Ab-initio investigations on elastic properties in $L1_2$ structure Al_3Sc and Al_3Y under high pressure", *J. of Alloys Compd.*, **585**, pp. 587-593 (2014).

20. Hu, W.C., Liu, Y., Li, D.J., Zeng, X.Q. and Xu, C.S. "Mechanical and thermo-dynamic properties of Al.sub.3Sc and Al.sub.3Li precipitates in Al-Li-Sc alloys from first-principles calculations", *Physica B*, **427**, pp. 85-90 (2013).

Biographies

Zohreh Ebrahimi received the BE degree in Mechanical Engineering from Shiraz University in 2004 and the MSc degree in Mechanical Engineering from Stuttgart University, Germany, in 2007. She has performed her Master Thesis in conjugation with German Aerospace Center (DLR) in Stuttgart. She received her PhD degree from RWTH Aachen University of Technology in November 2010 in Germany; her thesis was on development of a micromechanical phase-field model of eutectic growth. She is an expert in the area of phase-field modeling and has a variety of publications in this respect. Since January 2011, she has joined the Department of Engineering at Payame Noor University where she is currently an Assistant Professor in Mechanical Engineering group. Her research interests include different applications of the phase-field model, modeling and simulation, finite element modeling, damage and impact mechanics, fracture mechanics during fatigue and creep, elasticity and plasticity in material systems, and micro- and nano-mechanics.

Hosein Ebrahimi received the BE degree in Material Science and Engineering from Shiraz University in 2013. He was awarded as the best student as he graduated from Shiraz University. He received the MSc degree from Sharif University of Technology in Tehran, in December 2015, in the Department of Material Science and Technology; he obtained the highest records in his studies. His main research interests include modeling of material systems, finite element modeling, numerical simulations, metal forming, and material characterization.